Available online at www.sciencedirect.com
SCIENCE DIRECT
Biochimica et Biophysica Acta 1708 (2005) 219 – 228
BIOCHIMICA ET BIOPHYSICA ACTA
BBA
http://www.elsevier.com/locate/bba

Extinction coefficients and critical solubilisation concentrations of photosystems I and II from *Thermosynechococcus elongatus*

Frank Müh[a], Athina Zouni[b,*]

[a]*Institut für Experimentalphysik, Freie Universität Berlin, Arnimallee 14, 14195 Berlin, Germany*
[b]*Max-Volmer-Laboratorium für Biophysikalische Chemie, Technische Universität Berlin, Strasse des 17. Juni 135, 10623 Berlin, Germany*

Received 29 December 2004; received in revised form 10 March 2005; accepted 13 March 2005
Available online 1 April 2005

Abstract

The absorption properties of chlorophyll *a* (Chl*a*) in active core complexes of photosystems I (PSI) and II (PSII) isolated in high purity from the thermophilic cyanobacterium *Thermosynechococcus elongatus* were correlated with those of extracts in 80% acetone to determine effective extinction coefficients of protein-bound Chl*a* and molar extinction coefficients of core complexes and reaction centers (RC). These coefficients allow a quick determination of Chl*a* and protein concentrations from steady-state absorption spectra of intact samples without the need for pigment extraction and protein destruction. In the visible range, $\varepsilon^{p}_{680} = 57\ \mathrm{mM}^{-1}\ \mathrm{cm}^{-1}$ for trimeric PSI (PSIt) and $\varepsilon^{p}_{674} = 70\ \mathrm{mM}^{-1}\ \mathrm{cm}^{-1}$ for dimeric (PSIId) and monomeric (PSIIm) PSII (error ±6%; superscript "*p*" refers to Chl*a* bound to intact protein, subscripts are the peak maxima in nm). The integral extinction coefficient $\phi^{p} = 2.8\ \mathrm{nm}\ \mu\mathrm{M}^{-1}\ \mathrm{cm}^{-1}$ for the wavelength interval between 550 and 800 nm and the extinction coefficient $\varepsilon^{p}_{B} = 14\ \mathrm{mM}^{-1}\ \mathrm{cm}^{-1}$ for the smaller absorption maximum (B = 632 nm for PSI and 627 nm for PSII) were found to be essentially the same for both types of PS. The coefficients of PSIt are shown to remain unaltered when 65% (v/v) of the buffer is replaced with glycerol. Molar extinction coefficients of core complexes were determined using Chl*a*/RC ratios of 96±1 for PSI and 35±2 for PSII based on X-ray data. In addition, the critical solubilisation concentration of *n*-dodecyl-β-D-maltoside (βDM), necessary to keep the core complexes in solution, was determined by turbidimetric titrations. It was found that at least ~500 βDM molecules per PSIt (~2 βDM per Chl*a*) and 190 βDM molecules per PSIIm (~5 βDM per Chl*a*, also for PSIId) in excess of the critical micelle concentration of 0.16 ± 0.03 mM are necessary for a complete solubilisation of the core complexes.

Keywords: Chlorophyll determination; Critical solubilisation concentration; Detergent–protein ratio; Extinction coefficient; Photosystem I; Photosystem II

1. Introduction

In the photosynthesis carried out by cyanobacteria, algae and plants, two large membrane-embedded pigment–protein complexes (PPCs), called photosystem (PS) I and II, catalyse the processes of photochemical energy conversion [1]. Each PS core complex consists of a reaction center (RC), in which the light-induced electron transfer reactions take place, and a core antenna system transferring the energy from captured photons to the RC. PSI uses the light energy to reduce ferredoxin [2,3], which is required to produce NADPH for use in carbon metabolism. The electrons for this process are delivered from PSII mediated by water-soluble cytochrome c_6 or plastocyanin as well as the membrane embedded cytochrome $b_6 f$ complex and the plastoquinone pool. The photochemistry in PSII leads to reduction of plastoquinone with the required electrons originating from water oxidation at a manganese cluster under release of molecular oxygen [4].

Abbreviations: Chl, chlorophyll; CMC, critical micelle concentration; CSC, critical solubilisation concentration; βDM, *n*-dodecyl-β-D-maltoside; Pheo, pheophytin; PS, photosystem; PSIt, trimeric photosystem I core complex; PSIIm, monomeric photosystem II core complex; PSIId, dimeric photosystem II core complex; PPC, pigment–protein complex; RC, reaction center

* Corresponding author. Fax: +49 30 31421122.
E-mail address: zouni@phosis1.chem.tu-berlin.de (A. Zouni).

0005-2728/$ - see front matter © 2005 Elsevier B.V. All rights reserved.
doi:10.1016/j.bbabio.2005.03.005

In recent years, great progress has been made in determining the spatial structures of membrane proteins of oxygenic photosynthesis [5–12]. In particular, the X-ray structures of trimeric PSI (PSIt) and dimeric PSII (PSIId) core complexes isolated from the thermophilic cyanobacterium *Thermosynechococcus elongatus* were determined to resolutions of 2.5 Å [5] and 3.2 Å [12], respectively. Each monomeric part of PSIt consists of 12 different protein subunits (PsaA-F, PsaI-M, and PsaX) and 127 cofactors (96 chlorophylls (Chl*a*), 2 phylloquinones, 3 Fe_4S_4 clusters, 22 carotenoids, and 4 lipids). According to the most recent analysis [13], both the monomeric and the dimeric form of PSII from *T. elongatus* contain at least 19 different protein subunits (PsbA-F, PsbH-M, PsbO, PsbT-V, and PsbX-Z). Extensive chemical characterisation of these samples indicates the presence of approximately 36 Chl*a*, 9 carotenoids, 2 plastoquinones, 4 Mn, and 10–18 lipids per 2 pheophytins *a* (Pheo*a*) [14]. This is partially in accordance with results from X-ray crystallography of PSIId, where 36 Chls and 7 carotenoids per 2 Pheo*a* have been assigned on the basis of the 3.5 Å structure [11] and 35 Chls and one carotenoid based on the 3.2 Å data [12]. The isolated core complexes also bind detergent (*n*-dodecyl-β-D-maltoside, βDM), which is not resolved in the X-ray structure. Chemical analyses suggest the presence of about 150 βDM molecules per PSIIm, 220 per PSIId, and 500 per PSIt [14,15].

The analysis of the functional properties of isolated photosystems and the improvement of their crystal structures obviously require a combination of biochemical, physicochemical, and spectroscopic approaches [13–15]. In most of these studies, two pieces of information should be available, the importance of which is sometimes overlooked. One is the extinction coefficient of protein-bound Chl necessary to determine the molar concentration of the PPC under study. The other is the optimal concentration of detergent in the samples, which should not be too low to avoid protein aggregation and not too high to minimize detergent-induced artifacts.

While molar extinction coefficients for the RCs of anoxygenic photosynthesis have been determined [16,17], this appears not to be the case for PSI and PSII. The usual procedure of determining the PPC concentration is to extract the Chls from the protein scaffold using organic solvents followed by spectrometric quantification of Chl in the extract. The molar PPC concentration can then be calculated, provided the number of Chls per RC is known from spectroscopic studies of redox reactions in the RC [18,19]. Absolute extinction coefficients that would allow for a direct determination of the PPC concentration from simple steady-state spectra of dark-adapted samples are apparently not in use, as a variation of the number of Chls per RC between different preparations renders this approach less appropriate for quantitative determinations than difference spectroscopy of functional cofactor states in the RC. However, growing single crystals implies that the preparations are homogeneous and have only little contamination by unspecifically bound Chl. This fact should allow a quick and still reasonably accurate in situ-determination of the PPC concentration on the basis of the absorption spectrum and motivated us to determine the molar extinction coefficients of PSI and PSII from *T. elongatus* prepared under conditions where crystals are reproducibly obtained.

The extinction coefficients can be used only under conditions, where the Beer–Lambert law holds, i. e. for diluted, homogeneous, non-scattering solutions. Aqueous solutions of membrane proteins must contain a detergent at concentrations above a certain value to ensure proper solubilisation. We call this value the critical solubilisation concentration (CSC) to distinguish it from the critical micelle concentration (CMC). The CSC is higher than the CMC and depends linearly on the concentration of the membrane protein [20–22]. In order to optimise the use of βDM as solubilising agent in PSI and PSII samples, we also determined the parameters describing the linear dependence of the CSC on the PPC concentration.

2. Materials and methods

2.1. Protein isolation

Cells of *T. elongatus* were grown, thylakoids isolated, and the membrane proteins extracted with βDM and separated by weak anion exchange chromatography as described [14]. PSII containing fractions from the first column were separated into PSIIm (monomeric) and PSIId (dimeric) by a second column step [14]. PSIt (trimeric) eluting from the first column was further purified with Q-Sepharose HP (Pharmacia) in 20 mM MES (pH 6.4), 0.02% βDM using a linear gradient of $MgSO_4$ from 25 to 150 mM [23]. The samples were characterised by SDS-PAGE, measurement of flash-induced oxygen evolution of PSII [14] and MALDI-TOF mass spectrometry [13].

2.2. Optical correlation experiments

The buffer used for optical spectroscopy of intact PPCs contained 20 mM MES (pH 6.4), 25 mM $MgSO_4$, and 0.02% (w/v) βDM. Since a lot of experiments require the addition of glycerol as cryoprotectant or glass forming agent, glycerol was added to some samples to a final concentration of 65% (v/v). Absorption spectra were recorded with a Cary 50 spectrophotometer (Varian) using cuvettes with 1 cm path length. The absorption intensities were measured with baseline correction relative to the absorption at 800 nm. All experiments were performed at 22 °C with the temperature controlled via a home-built cuvette holder connected to a Haake K thermostat.

Chl*a* extracts were obtained by diluting the protein stock solution in a buffer/acetone mixture to give 80% (v/v) acetone, vortexing, and removing the denatured protein by

centrifugation. To study the correlation of Chl absorption between buffered and acetone-extracted solutions, a certain volume of the protein stock solution (corresponding to about 200 μM Chl*a*) was diluted in either buffer or buffer/acetone mixture to give 1 mL of solution in each case, resulting in a pair of samples with the same Chl concentration. This procedure was followed for a number of different PPC concentrations with material from three different protein preparations for each type of PPC. All experiments were carried out under dim green light to minimize light-induced degradation of extracted Chl*a* [24].

2.3. Calculation of extinction coefficients

According to the Beer–Lambert law the measured absorption A_λ^e of Chls in a certain environment (where the index e for "environment" is replaced in the following by a for 80% acetone and p for intact PPCs) at a wavelength λ (in nm) is proportional to the optical path length d and the total molar concentration c_{Chl} of the Chls in the sample:

$$A_\lambda^e = d\varepsilon_\lambda^e c_{\mathrm{Chl}}. \tag{1}$$

The proportionality constant ε_λ^e is the (decadic) molar extinction coefficient (in $\mathrm{M^{-1}\ cm^{-1}}$). Alternatively, one may use the specific extinction coefficient α_λ^e (in $\mathrm{L\ g^{-1}\ cm^{-1}}$). In the following $d = 1$ cm and we neglect it in the formulae.

If a certain volume of a protein stock solution is diluted by the same factor in either buffer or acetone/buffer mixture as described above, the measured absorptions of the two samples correspond to essentially the same total concentration of Chl*a*. Accordingly, the integrals

$$F^e = \int_{\lambda_1}^{\lambda_2} A_\lambda^e d\lambda \tag{2}$$

over a suitably chosen wavelength interval $[\lambda_1,\lambda_2]$ should be the same for both samples, provided environmental effects on the oscillator strength of the Chls can be neglected. As shown below, this is approximately the case for $\lambda_1 = 550$ nm and $\lambda_2 = 800$ nm. However, due to the different microenvironments and mutual excitonic interactions of the Chls in the protein compared to the acetone-extract, the oscillator strength will be distributed differently over the wavelength interval in the two cases. Thus, for any two wavelengths λ_a and λ_p we have in general

$$A_{\lambda_p}^p = R_{\lambda_a}^{\lambda_p} A_{\lambda_a}^a, \tag{3}$$

where the proportionality constant $R_{\lambda_a}^{\lambda_p}$ can be determined by linear regression. Knowing $R_{\lambda_a}^{\lambda_p}$, one can calculate the Chl*a* content of a sample directly from the optical absorption of the intact protein by using the effective extinction coefficients:

$$\varepsilon_{\lambda_p}^p = R_{\lambda_a}^{\lambda_p} \varepsilon_{\lambda_a}^a, \tag{4}$$

$$\alpha_{\lambda_p}^p = R_{\lambda_a}^{\lambda_p} \alpha_{\lambda_a}^a, \tag{5}$$

where $\varepsilon_{\lambda_a}^a$ and $\alpha_{\lambda_a}^a$ are known from the literature [24]. For the band A absorption maximum of Chl*a* in 80% acetone at 664 nm (cf. Fig. 1), we have (neglecting effects from solutes in the 20% buffer, which have no measurable effect on the absorption spectra between 550 and 800 nm): $\varepsilon_{664}^a = (7.68 \pm 0.04)\ 10^4\ \mathrm{M^{-1}\ cm^{-1}}$ and $\alpha_{664}^a = (86.0 \pm 0.5)\ \mathrm{L\ g^{-1}\ cm^{-1}}$. These coefficients were determined with A_{750} set to zero [24], which is equivalent to our setting of $A_{800} = 0$. There is also a linear relationship between the integral F^p ($\lambda_1 = 550$ nm, $\lambda_2 = 800$ nm) and the absorption intensity of the acetone extract at a particular wavelength:

$$F^p = Q_{\lambda_a} A_{\lambda_a}^a. \tag{6}$$

This allows for a direct calculation of the Chl*a* content from the integral by using the integral extinction coefficients:

$$\phi^p = Q_{\lambda_a} \varepsilon_{\lambda_a}^a, \tag{7}$$

$$\varphi^p = Q_{\lambda_a} \alpha_{\lambda_a}^a. \tag{8}$$

Note that these coefficients are defined in wavelength units for convenience. Integral extinction coefficients are often defined in wave number or frequency units and then are proportional to the oscillator strength.

If the number N_{Chl} of Chls bound to one protein complex is known, the molar concentration of the complex, $c_{\mathrm{PPC}} = c_{\mathrm{Chl}}/N_{\mathrm{Chl}}$, can be calculated. For the molar extinction coefficient of the PPC, we obtain from Eq. (4):

$$\varepsilon_{\lambda_p}^{\mathrm{PPC}} = N_{\mathrm{Chl}} \varepsilon_{\lambda_p}^p = N_{\mathrm{Chl}} R_{\lambda_a}^{\lambda_p} \varepsilon_{\lambda_a}^a \tag{9}$$

and similarly for the other coefficients. Eq. (9) is valid for any wavelength λ_p, where only Chl*a* absorbs. Thus, the molar extinction coefficient of the PPC can be determined for different wavelengths λ_p from $R_{\lambda_a}^{\lambda_p}$ and N_{Chl} using $\varepsilon_{\lambda_a}^a$ for one wavelength λ_a (e.g., 664 nm) as the calibration

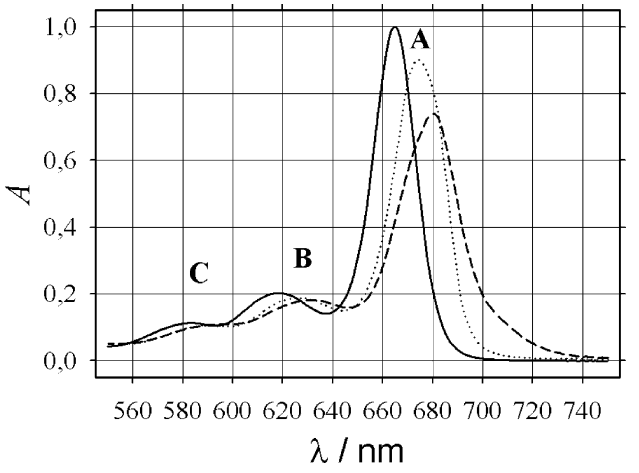

Fig. 1. Optical absorption spectra of Chl*a* in 80% acetone (solid), PSIt (dashed), and PSIId (dotted) normalized to a Chl*a* concentration of 13 μM ($A_{664}^a = 1$) such that for the PPC spectra $A_{\lambda_p}^p = R_{664}^{\lambda_p}$ and $F^p = Q_{664}$. Letters A, B, C label the three absorption maxima observed for each spectrum between 550 and 800 nm.

standard. Finally, one may calculate an effective molar extinction coefficient of the RCs via

$$\varepsilon_{\lambda_p}^{\mathrm{RC}} = \varepsilon_{\lambda_p}^{\mathrm{PPC}} / N_{\mathrm{RC}}, \tag{10}$$

where N_{RC} is the number of RCs in the PPC (i.e., 1 for monomers, 2 for dimers, etc.).

2.4. BioBeads treatment and determination of CSC

Detergent was removed by a BioBeads treatment similar to the methods of Gast et al. [20,21,25]. PSIt solutions corresponding to 3 mM Chl*a* in 20 mM MES (pH 6.4), 0.02% βDM and 50 mM $MgSO_4$ were diluted with 5 mM MES (pH 6.4) to 75 μM Chl*a* and incubated on a shaker with 0.15 g/mL BioBeads SM2 (Biorad) at 4 °C in the dark for 45 min. The suspension was filtered to remove the BioBeads and centrifuged at 3000 × g for 15 min. at 4 °C. The pellet was resuspended in 5 mM MES (pH 6.4), stored in the dark at 4 °C and used within a few days. In the case of PSII samples we started with solutions of 4 mM Chl*a* in either 40 mM MES (pH 6.0), 0.02% β-DM, 5% (w/w) glycerol, 20 mM $CaCl_2$, 25 mM $MgSO_4$ (PSIIm) or 100 mM PIPES (pH 7.0), 0.03% β-DM, 5 mM $CaCl_2$ (PSIId), which were diluted to 40 μM Chl*a* with 20 mM MES (pH 6.4) and incubated with 0.1 g/mL BioBeads. The detergent-depleted PSII, resuspended in 5 mM MES (pH 6.4), was also stored at 4 °C, but used within 1 day.

To determine the CSC, detergent-depleted PPCs were suspended in 5 mM MES (pH 6.4), 50 mM $MgSO_4$ to give maximally ~60 μM Chl *a* (PSI) or in 5 mM MES (pH 6.4), 2 mM $CaCl_2$ to give maximally ~20 μM Chl *a* (PSII). The suspension was then titrated with a solution of 0.5% (9.79 mM) βDM and the extinction monitored at 550 nm (E_{550}). Upon solubilisation E_{550} drops due to the clarification of the sample. The CSC (termed c_{sol} in [22]) can be determined from a plot of E_{550} against the concentration of added detergent ($c_{\beta\mathrm{DM}}$) as the point, where E_{550} reaches its minimum level (see below), and is a linear function of the protein concentration c_{PPC} according to

$$\mathrm{CSC} = n_0\ c_{\mathrm{PPC}} + c_0. \tag{11}$$

The parameter c_0 is practically identical to the CMC of the detergent as given in the literature (measured in protein-free aqueous solutions). n_0 is the number of detergent molecules per PPC that must be present in the solution in excess of the CMC in order to ensure solubilisation of the protein. The CSC can also be given as a function of the molar Chl*a* concentration:

$$\mathrm{CSC} = n_1\ c_{\mathrm{Chl}} + c_0, \tag{12}$$

where $n_1 = n_0/N_{\mathrm{Chl}}$. PPC and Chl*a* concentrations of clarified samples were determined using the band B extinction coefficients determined in this work (Table 1).

3. Results and discussion

3.1. Correlation of absorption properties

Chl*a* gives rise to characteristic absorptions in the visible range. Three bands can be resolved in the region from 550 to

Table 1
Proportionality constants describing the correlation of the absorption of Chl*a* in PSI and PSII samples with that in 80% acetone as defined in Eqs. (3) and (6) and extinction coefficients calculated according to Eqs. (4), (5) and Eqs. (7)–(10)

Sample	PSIt	PSIt in 65% (v/v) glycerol	PSIIm	PSIId
# data points	144	148	169	145
F^p/F^a	1.060±0.013	1.058±0.014	1.047±0.013	1.021±0.012
Q_{664}/nm	36.62±0.30	37.37±0.41	36.95±0.38	35.98±0.38
R_{664}^{A}	0.743±0.006	0.740±0.008	0.919±0.008	0.900±0.008
R_{664}^{B}	0.178±0.002	0.181±0.002	0.196±0.002	0.186±0.002
ϕ^p/nm μM^{-1} cm^{-1}	2.81±0.04	2.87±0.05	2.84±0.05	2.76±0.05
φ^p/nm L mg^{-1} cm^{-1}	3.15±0.05	3.21±0.06	3.18±0.05	3.09±0.05
$\varepsilon_{\mathrm{A}}^p$/mM^{-1} cm^{-1}	57.1±0.8	56.8±0.9	70.6±1.0	69.1±1.0
$\varepsilon_{\mathrm{B}}^p$/mM^{-1} cm^{-1}	13.7±0.3	13.9±0.3	15.1±0.3	14.3±0.3
α_{A}^p/L g^{-1} cm^{-1}	63.9±0.9	63.6±1.1	79.0±1.1	77.4±1.1
α_{B}^p/L g^{-1} cm^{-1}	15.3±0.3	15.6±0.3	16.9±0.3	16.0±0.3
N_{Chl}	288±3	288±3	37±2	74±4
ϕ^{PPC}/nm nM^{-1} cm^{-1}	0.81±0.02	0.83±0.03	0.11±0.01	0.20±0.02
$\varepsilon_{\mathrm{A}}^{\mathrm{PPC}}$/μM^{-1} cm^{-1}	16.4±0.4	16.4±0.5	2.6±0.2	5.1±0.4
$\varepsilon_{\mathrm{B}}^{\mathrm{PPC}}$/μM^{-1} cm^{-1}	3.95±0.13	4.00±0.13	0.56±0.05	1.06±0.08
N_{RC}	3	3	1	2
ϕ^{RC}/nm nM^{-1} cm^{-1}	0.27±0.01	0.28±0.01	0.11±0.01	0.10±0.01
$\varepsilon_{\mathrm{A}}^{\mathrm{RC}}$/μM^{-1} cm^{-1}	5.5±0.2	5.5±0.2	2.6±0.2	2.6±0.2
$\varepsilon_{\mathrm{B}}^{\mathrm{RC}}$/μM^{-1} cm^{-1}	1.32±0.04	1.33±0.05	0.56±0.05	0.53±0.04

Integrals were taken between 550 and 800 nm. Index "A" represents the peak maxima of band A at 680 and 674 nm for PSI and PSII samples, respectively, while "B" designates the maxima of band B at 632 and 627 nm, respectively. The given errors of parameters obtained by linear regression of experimental data are standard deviations of fits involving the given number of data points. These include data from three different preparations for each type of sample. The error margins of calculated data include in addition the error of ε_{664}^a given by Porra et al. [24]. The number N_{Chl} is deduced from X-ray data (2.5 Å for PSIt [5] and 3.2 Å for PSIId [12], including Pheo*a*). N_{RC} follows from size exclusion chromatography as described in [15].

750 nm for Chl*a* in 80% acetone with maxima at 664, 618 and 583 nm and relative peak intensities of 4.8:1:0.56. The most intense of these bands is usually assigned to the Q_Y transition according to Gouterman's four orbital model [26], but the assignment of the other two bands is less clear [27, 28]. Therefore, we shall designate these bands as A, B, C, respectively, rather than Q_Y, Q_X, etc. In the spectra of the PPCs, these three bands can also be found, but are significantly redshifted compared to Chl*a* in solution (Fig. 1).

In order to correlate the absorption properties of protein-bound Chl*a* with those of Chl*a* in 80% acetone, we recorded the spectra of concentration-correlated pairs of buffered and acetone-extracted samples (prepared as described in Section 2.2) under identical spectroscopic conditions. The total number of sample pairs (# data points) for each type of sample is given in Table 1 and ranges between 144 and 169, while one individual measurement series involves between 21 and 28 data points. We investigated three types of PPCs: Trimeric PSI (PSIt) and dimeric PSII (PSIId), which could be crystallised [5,6,12,14], and in addition a fraction of the PSII preparation, which on the basis of [15] can be attributed to monomeric PSII (PSIIm).

Representative spectra of PSIt and PSIId are shown in Fig. 1 together with the spectrum of the corresponding acetone-extract. The spectrum of PSIIm is similar to that of PSIId, and the two Pheo*a* per RC present in PSII cannot be resolved in the spectra. For the correlation of absorption integrals we chose λ_1 = 550 nm as the lower integration limit for two reasons: First, all spectra have minimal absorption in this region, so that errors due to the cut-off are small. Second, only Chl*a* (and Pheo*a*) absorb in the region above 550 nm (neglecting possible small contributions from cytochromes present in PSII and carotenoids). To avoid any further cut-off, the upper integration limit was set to λ_2 = 800 nm.

Fig. 2A shows that the ratio F^p/F^a of the integral for the intact PPC and that of the acetone-extract is close to, but in

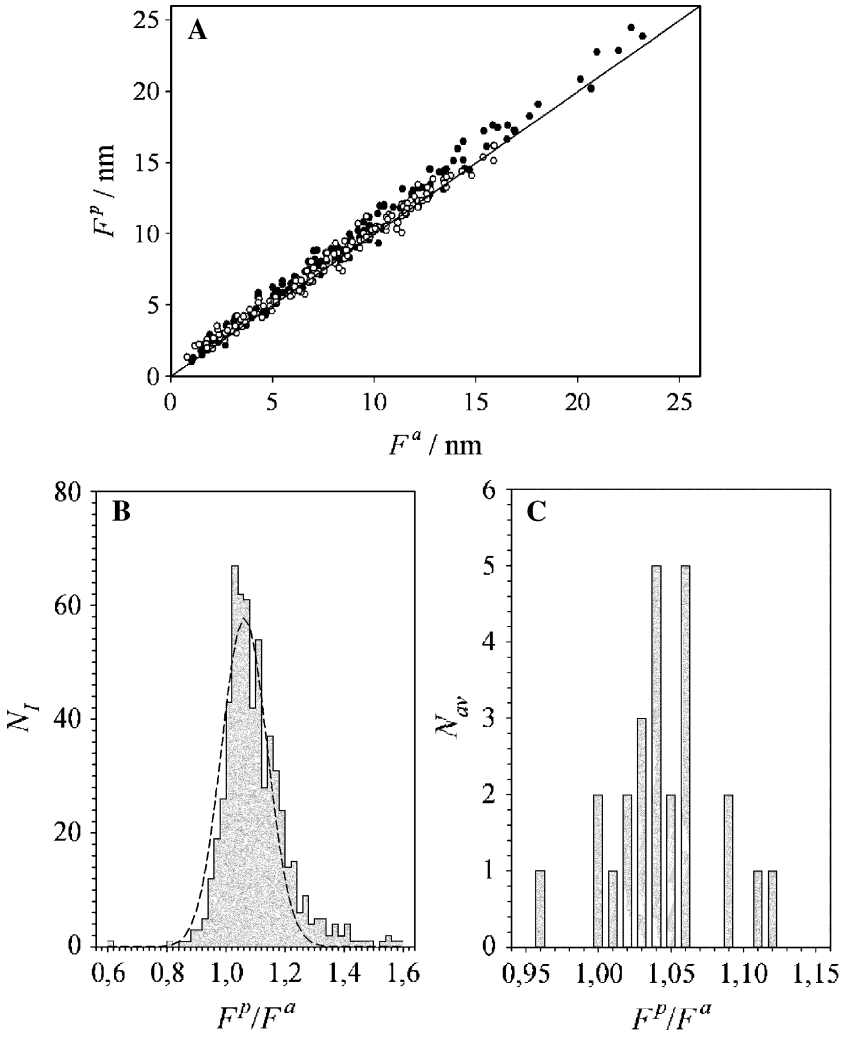

Fig. 2. (A) Correlation of the absorption integral F^p between 550 and 800 nm of PSIt (●) and PSIId (○) with the corresponding integral F^a of the acetone-extracts. The straight line corresponds to $F^p = F^a$. (B) Frequency distribution N_I of the ratio F^p/F^a of all 606 individual concentration-correlated sample pairs (both PSI and PSII) for a bin size of I = 0.02. The dashed curve represents a Gaussian distribution with center 1.06 and width 0.2. (C) Frequency distribution N_{av} of the ratio F^p/F^a averaged over single measurement series with 21 to 28 data points for a bin size of 0.01.

general not equal to one. Linear regression yields values of 1.06 for PSIt and somewhat smaller values for PSIIm and PSIId (Table 1). The latter deviation is probably not significant in view of the scattering of the data as apparent from Fig. 2A. This can be seen even more clearly from the different type of analysis presented in Fig. 2B. Here, we calculated the integral ratio explicitly for each individual sample pair and determined the frequency distribution of F^p/F^a values for a bin size of 0.02 (i.e., for $F^p/F^a = 1.00$, N_I counts the number of F^p/F^a values falling into the range $1.00 \leq F^p/F^a < 1.02$). The distributions are indeed not significantly different for the various sample types, so that we do not distinguish between PSI and PSII in Fig. 2B. A best fit of the frequency distribution of all 606 sample pairs to a Gaussian yields a center at 1.06 and a width of 0.20. The asymmetry of the distribution shown in Fig. 2B is not significant as follows from analyses of frequency distributions with different bin sizes.

It is instructive to see what happens, if only a smaller number of data points is analysed. Thus we determined the frequency distribution N_{av} of F^p/F^a ratios corresponding to single measurement series with 21 to 28 data points (Fig. 2C). The ratios varied between 0.96 and 1.12, but the frequency distribution peaks around 1.05. This demonstrates that the analysis of a smaller number of sample pairs can be misleading and that about 100 to 150 data points are required for a reliable determination of proportionality constants. This relatively large scattering of F^p/F^a ratios is neither due to pipetting errors nor does it reflect differences between individual preparations. Also, variation of the incubation time in 80% acetone has no significant effect on this error. We suggest that coprecipitation of loosely bound pigments with the denatured protein in the centrifugation step could be a source of uncertainty, which is difficult to control.

Fig. 3 shows examples of the linear correlation of the integral F^p (A) and the absorption intensity A^p at different peak maxima (B) of intact PPCs with the absorption A^a of the corresponding acetone-extract at 664 nm. The latter is used here as calibration standard and provides proportionality constants Q_{664} and $R_{664}^{\lambda_p}$ (Table 1) for the calculation of effective extinction coefficients. For Q_{664}, we obtain the same value for PSIt and PSIIm. The somewhat smaller value for PSIId (Table 1) indicates no significant deviation in view of the above analysis of the F^p/F^a ratios. A similar argument applies to the band B maximum of the PPCs, which has 18% of the intensity of the band A maximum of the acetone-extract for PSI and 19% for PSII. Thus, the only important difference between PSI and PSII is in the constant R_{664}^{A}, which implies that the band A maximum is decreased to 74% in PSI, but only to 90% in PSII as compared to acetone. These latter constants were used to scale the spectra in Fig. 1. Hence, the constants for other wavelengths can directly be read from the figure.

It is of particular practical interest that replacing 65% of the solution volume with glycerol has no effect on the key parameters F^p/F^a, Q_{664}, R_{664}^{A}, and R_{664}^{B} for PSIt (Table 1).

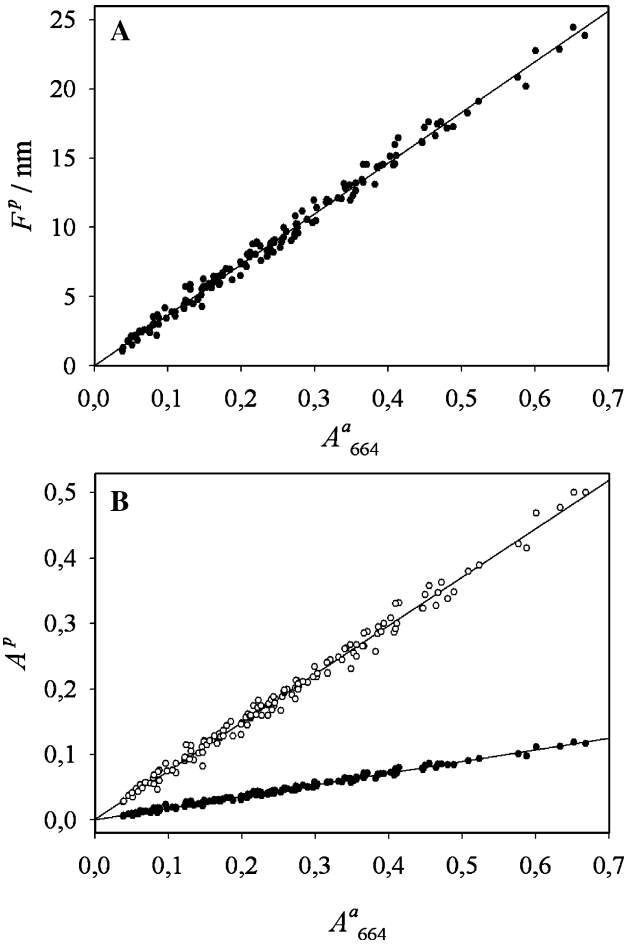

Fig. 3. (A) Linear correlation of the absorption integral F^p between 550 and 800 nm of PSIt with absorption intensity A^a of band A (664 nm) of the acetone-extracts. The slope is Q_{664}. (B) Linear correlation of the absorption intensity A^p of band A (○, 680 nm) and band B (●, 630 nm) of PSIt with A^a_{664}. The slopes are R_{664}^{A} and R_{664}^{B}, respectively.

This implies that the Chl*a* concentration of glycerol containing samples can be assayed spectroscopically (at 22 °C) in the same way as for glycerol-free samples. Although we did not explicitly investigate the effects of glycerol on the gross absorption properties of PSII samples in this work, we assume that they are likewise negligible concerning the Chl*a* determination.

3.2. Effective extinction coefficients of Chla

Knowing the proportionality constants Q_{664}, R_{664}^{A}, and R_{664}^{B}, the effective extinction coefficients of the Chls in intact PPCs can be calculated according to Eqs. (4), (5), (7), and (8). As an example, we obtain for the molar extinction coefficients corresponding to the band A maximum 57 mM^{-1} cm^{-1} for PSI and 70 mM^{-1} cm^{-1} for PSII as compared to 76.8 mM^{-1} cm^{-1} for Chl*a* in 80% acetone (Table 1). These values reflect the reduction of the peak intensities of the PPC samples apparent from Fig. 1. As a result of the above analysis, the integral extinction coefficients ϕ^p and φ^p are essentially the same for both types of core complexes. The

extinction coefficients for the band B maximum are also nearly the same for PSI and PSII, although they refer to different wavelengths. This suggests that ϕ^{P}, φ^{P}, ε^{p}_{B}, and α^{p}_{B} (Table 1) are independent of specific pigment–protein interactions. Consequently, these values may also be used for PSI and PSII samples from other organisms and even for other Chl*a*-binding proteins. All extinction coefficients have an error of about 6% corresponding to a 99% confidence interval. This error takes into account the scattering of the correlation plots (see Figs. 2A and 3A, B) and the error of ε^{a}_{664} given by Porra et al. [24].

In PSII, there are two Pheo*a* in the RC contributing to the absorption between 550 and 800 nm. Assuming that there are 35 Chl*a* and 2 Pheo*a* per RC (see below) and that they are all completely extracted by 80% acetone, the extinction coefficient of the extract at 664 nm can be written:

$$\varepsilon^{a}_{664}(\mathrm{PSII}) = 0.946\ \varepsilon^{a}_{664}(\mathrm{Chl}a) + 0.054\ \varepsilon^{a}_{664}(\mathrm{Pheo}a). \quad (13)$$

To determine the extinction coefficient of Pheo*a* we added 1 μL of 12.5% HCl to 1 mL of an acetone extract of PSIt, which contains Chl*a* only (concerning the absorption above 550 nm). This procedure converts Chl*a* almost exclusively to Pheo*a* [29]. The decrease of the absorption at 664 nm indicated that ε^{a}_{664} (Pheo*a*) = 0.58 ε^{a}_{664} (Chl*a*) (corresponding with [29]) and hence ε^{a}_{664} (PSII) = 0.98 ε^{a}_{664} (Chl*a*). It follows that treating the two Pheo*a* effectively as Chl*a* as we did causes an overestimation of the effective extinction coefficients by 2%.

3.3. Molar extinction coefficients of PPCs and RCs

The molar extinction coefficients of PPCs can be calculated from those of the Chls, if the number N_{Chl} of Chls bound to the PPC is known. The most recent structure refinements of core complexes from *T. elongatus* allow a reasonable estimate of this number. The 2.5-Å structure of Jordan et al. [5] suggests that N_{Chl} = 288 for PSIt. This value is in excellent agreement with 102±6 Chl*a*/RC determined by spectroscopic methods (oxidation of P_{700}) applied to the same material that was used for crystallisation [30]. Since the spectroscopic methods involve redox chemistry that has not absolutely a 100% yield, they may slightly underestimate the RC concentration and hence overestimate the Chl/RC ratio. We assume that the value of N_{Chl} deduced from the X-ray structure is reliable, but add a minimal error of ±1 Chl*a*/RC.

The most recent refinement of the X-ray structure of PSIId at 3.2Å resolution [12] shows 35 Chl*a* and 2 Pheo*a* per monomer. While the number of Chls and Pheos in the RC is certain, the number of Chls in the core antenna (CP43, CP47) still bears some uncertainty [11,12]. We estimate this error to ±2 Chl*a*/RC on the basis of the X-ray data. For comparison, Chl*a*/Pheo*a* ratios determined by reversed phase high pressure liquid chromatography give 34±2.2 Chl*a* per 2 Pheo*a* for both PSIId before and after crystallisation and 35±2.6 for PSIIm [14]. Thus, we use a total value of 37±2 pigments per RC (Table 1). This value is also in reasonable agreement with lower limits of Chl*a*/RC ratios determined from Q_A quantification and O_2 evolution activity [14].

The number N_{Chl} of pigments per PPC is related to the number N_{RC} of core complexes that form a tightly bound super complex (i.e., the number of RCs present in one super complex). This number can be determined by several methods as shown in [15]. In the present paper, we use the data obtained from size exclusion chromatography, which confirm that PSIt, PSIIm and PSIId are indeed trimers, monomers, and dimers, respectively, in the investigated range of Chl*a* concentrations [15].

3.4. Critical solubilisation concentrations

A typical spectrum of PSIt treated with BioBeads and resuspended in detergent-free buffer is shown in Fig. 4A

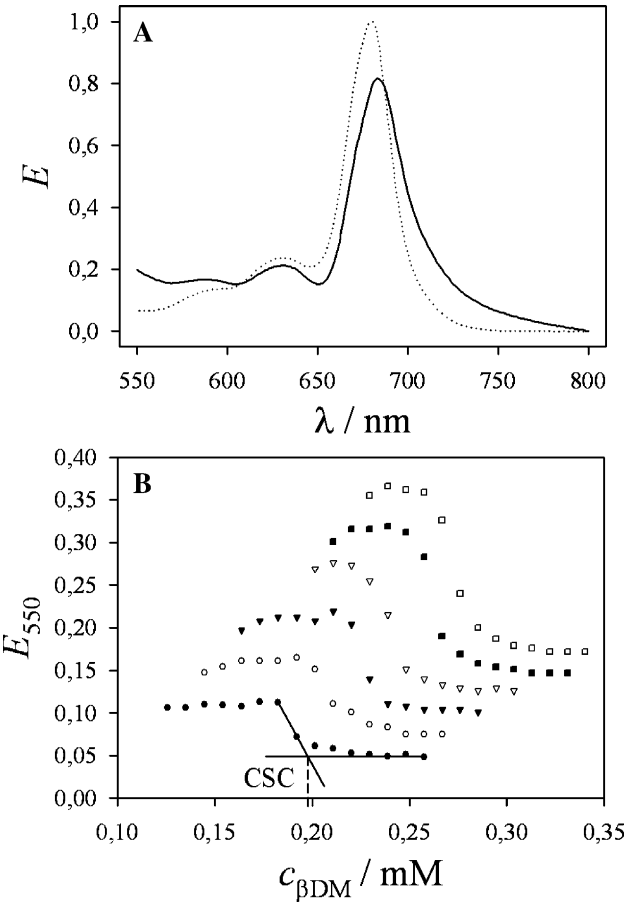

Fig. 4. (A) Spectrum of PSIt after BioBeads treatment and resuspension in 5 mM MES (pH 6.4), 50 mM $MgSO_4$ (solid) compared to PSIt solubilised with 0.02% βDM in the same buffer (dotted). (B) Dependence of the extinction E at 550 nm (due to absorption and scattering) upon the concentration of added βDM for six PSIt samples corresponding to Chl*a* concentrations between 55 and 110 μM. The extrapolation procedure for CSC determination (as described in 3.4) is indicated for the lowermost titration curve, for which CSC = 0.195 mM.

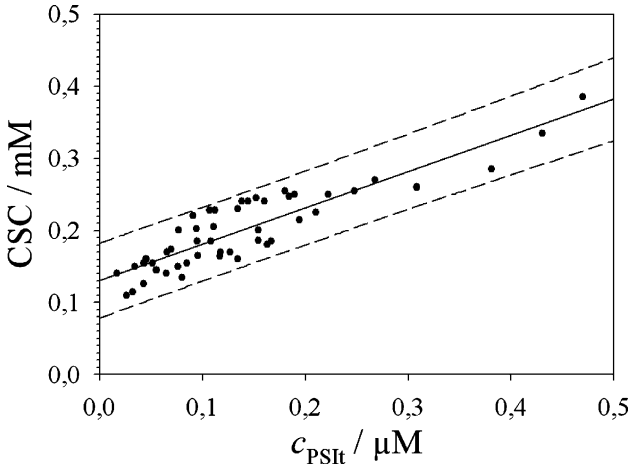

Fig. 5. Dependence of the CSC of βDM for PSIt on the PPC concentration in 5 mM MES (pH 6.4), 50 mM $MgSO_4$ at 22 °C. The solid line is a linear fit according to Eq. (11) yielding $c_0 = 0.13 \pm 0.01$ mM and $n_0 = 500 \pm 40$ (Table 2). The dashed lines indicate the 95% prediction interval for CSC as a function of c_{PSIt}. For $c_{PSIt} \rightarrow 0$ CSC approaches the CMC, which for βDM can be estimated to be 0.13 ± 0.05 mM.

(solid curve). Since such a sample is turbid, the apparent extinction E is the sum of two contributions, light scattering and absorption. The scattering contribution is particularly evident in regions of the spectrum, where the absorption is minimal, and causes an increase of E compared to the scatter-free solution of the solubilised PPC (dotted in Fig. 4A). The absorption itself does not follow the Beer–Lambert law, but is distorted with respect to scatter-free samples due to flattening of the absorption maxima [31], which is evident for both band A and B. The flattening is due to aggregation of the absorbing entities as a consequence of detergent removal and centrifugation. Both effects, scattering and flattening, vanish upon addition of detergent at concentrations above the CSC.

The recovered absorption spectrum is similar to the original spectrum of the freshly prepared sample. MALDI-TOF spectra indicate that detergent depletion with BioBeads is accompanied by a loss of PsaJ and possibly also PsaK, which on the basis of the X-ray structure [5] can be expected to cause the removal of 3–5 peripheral antenna Chls. Since these subunits are small (1–2 transmembrane helices), their loss should have no large effect on the number of detergent molecules necessary to resolubilise PSIt.

The differences between the spectra in Fig. 4A can be used to monitor the resolubilisation, e.g., at 550 nm. Typical titration curves of PSIt are shown in Fig. 4B. The initial extinction increases slightly with increasing βDM concentration followed by a sudden decrease and an asymptotic approach towards the extinction observed in scatter-free solutions. The slight increase of scattering is probably due to the dispersion of larger PPC aggregates into smaller ones, since it is accompanied by a reduction of the flattening effect, whereas the sudden decrease of scattering is interpreted as dissociation of the aggregates [20]. The asymptotic tail of the titration curve makes it difficult to define the detergent concentration, at which the solubilisation is completed. Therefore, the titration end point, i.e., the CSC, is determined by extrapolation of the steepest descent of the titration curve to the horizontal line representing the asymptotic value of E_{550} as indicated for the lowermost curve in Fig. 4B.

Apparently, the CSC depends on the concentration of PSIt (Fig. 4B). A plot of CSC versus the spectrophotometrically determined Chl*a* concentration (not shown) or the PPC concentration (Fig. 5) shows that this dependence is essentially linear in the investigated range of $c_{Chl} < 60$ µM. We do not know, whether the linearity also applies to higher Chl*a* concentrations. The values of c_0, n_0, and n_1 obtained from linear regression (Table 2) allow for a prediction of the CSC as a function of c_{PPC} or c_{Chl}, which due to the scattering of the data has an uncertainty of ±0.05 mM (95% prediction interval). Taking into account this uncertainty (which is larger than the standard deviation given in Table 2), the parameter c_0 – corresponding to the CSC extrapolated to $c_{PPC} = 0$ – is in good agreement with the CMC of βDM, reported in the literature to be between 0.16 and 0.19 mM [32]. Preliminary measurements using pyrene fluorescence [33] indicate that the CMC of βDM in 20 mM MES (pH 6.4) is ~0.15 mM and is practically independent of the $MgSO_4$ concentration between 0 and 50 mM (Müh, F., unpublished data).

The values of n_0 and n_1 indicate that at least 500 βDM molecules per PSI trimer or about two βDM molecules per (protein-bound) Chl*a* molecule must be present in excess of the CMC to keep the trimer solubilised. This is in excellent agreement with the number of 500 ± 100 detergent molecules per trimeric complex obtained from colorimetric quantification of the maltose head groups of βDM [15]. We also tried to quantify βDM in the detergent-depleted samples by this approach, but obtained so far only an upper limit of about 20% of detergent (and lipids) remaining bound to the PPC. Based on the experience of others with BioBeads-treatment [20], we think that the βDM concentration in the detergent-depleted samples is in fact much smaller (i.e., on the order of 5% of the original value), but may vary between samples. This uncertainty clearly contributes to the scattering of data and will cause an underestimation of the parameters c_0, n_0, n_1. Experiments to further optimise the BioBeads-treatment and improve the quantification of βDM in detergent-depleted samples are in progress.

Table 2
Parameters describing the dependence of the CSC of PSI and PSII samples on the PPC and Chl*a* concentration according to Eqs. (11) and (12)

sample	PSIt[a]	PSIIm[b]	PSIId[b]
c_0/mM	0.13±0.01	0.16±0.01	0.18±0.01
n_0	500±40	190±12	361±27
n_1	1.76±0.13	5.11±0.33	4.87±0.36

The given errors are standard deviations of fits with 10 to 50 datapoints corresponding to a 68% confidence interval. The 95% prediction interval for CSC as a function of c_{PPC} or c_{Chl} is on the order of ±0.05 mM.

[a] 50 mM $MgSO_4$.

[b] 2 mM $CaCl_2$.

All titration experiments with PSIt were performed in the presence of 50 mM $MgSO_4$, since we were not able to resolubilise detergent-depleted PSIt in the absence of electrolyte. Turbidimetric titrations of PSIt in 0.02% (0.39 mM) βDM with $MgSO_4$ (not shown) indicate that the $MgSO_4$ concentration for salting in PSIt increases linearly with c_{Chl}, ranging from 4 to 13 mM between 12 and 70 μM Chl*a* at pH 6.4. Preliminary experiments point to the possibility that the parameters n_0 and n_1 also depend on ionic strength between 20 and 50 mM $MgSO_4$, but the method is not accurate enough to draw definitive conclusions about the electrolyte dependence of these parameters. Complete solubilisation could also be achieved with 50 mM $CaCl_2$ instead of $MgSO_4$.

The detergent titration method was also applied to PSII preparations, corroborating earlier work of Hemelrijk [25]. The optical spectra of resolubilised PSIIm and PSIId were essentially the same as those of freshly prepared material (not shown). We observed a loss of oxygen evolution activity due to the BioBeads treatment, which on the basis of MALDI-TOF spectra can be traced back to the removal of PsbO. As with PSIt, we suggest that this modification of the protein sample should not strongly affect the CSC. It turns out that at least five βDM molecules per Chl*a* must be present in excess of the CMC to ensure proper solubilisation of both PSIIm and PSIId in the investigated range below 20 μM Chl*a* (Table 2). These values are in reasonable agreement with results from colorimetric quantification [14]. We found that 2 mM $CaCl_2$, which as a matter of routine is present in our PSII samples, suffices for a complete resolubilisation of PSIIm and PSIId at pH 6.4. Hence, the strong influence of ionic strength on the solubility as observed for PSIt appears to be absent in the case of PSII.

Acknowledgments

We thank R. Brunn (FU Berlin) for performing titrations and D. DiFiore and C. Lüneberg (both TU Berlin) for technical assistance with cell growth, protein isolation and purification. We are also grateful to Dr. J. Frank for his commitment in the preparation of PSIt samples and Dr. J. Kern for his help with PSII preparations and detergent/lipid analysis. Furthermore, we wish to thank Drs. E. Schlodder, K.-D. Irrgang (both TU Berlin) and Th. Renger (FU Berlin) for insightful discussions and comments and Profs. P. Hildebrandt (TU Berlin) and D. Stehlik (FU Berlin) for providing laboratory equipment. This work was supported by DFG (Sfb 498). Finally, we thank Dr. R. Clarke for careful reading of the manuscript.

References

[1] D.R. Ort, C.F. Yocum, Oxygenic Photosynthesis: the Light Reactions, Kluwer, Dordrecht, 1996.
[2] K. Brettel, Electron transfer and arrangement of the redox cofactors in photosystem I, Biochim. Biophys. Acta 1318 (1997) 322–373.
[3] K. Brettel, W. Leibl, Electron transfer in photosystem I, Biochim. Biophys. Acta 1507 (2001) 100–114.
[4] R.J. Debus, The manganese and calcium ions of photosynthetic oxygen evolution, Biochim. Biophys. Acta 1102 (1992) 269–352.
[5] P. Jordan, P. Fromme, H.T. Witt, O. Klukas, W. Saenger, N. Krauss, Three-dimensional structure of cyanobacterial photosystem I at 2.5 Å resolution, Nature 411 (2001) 909–917.
[6] A. Zouni, H.T. Witt, J. Kern, P. Fromme, N. Krauss, W. Saenger, P. Orth, Crystal structure of photosystem II from *Synechococcus elongatus* at 3.8 Å resolution, Nature 409 (2001) 739–743.
[7] N. Kamiya, J.R. Shen, Crystal structure of oxygen-evolving photosystem II from *Thermosynechococcus vulcanus* at 3.7 Å resolution, Proc. Natl. Acad. Sci. U. S. A. 100 (2003) 98–103.
[8] D. Stroebel, Y. Choquet, J.L. Popot, D. Picot, An atypical haem in the cytochrome b_6f complex, Nature 426 (2003) 413–418.
[9] A. Ben-Shem, F. Frolow, N. Nelson, Crystal structure of plant photosystem I, Nature 426 (2003) 630–635.
[10] Z. Liu, H. Yan, K. Wang, T. Kuang, J. Zhang, L. Gui, X. An, W. Chang, Crystal structure of spinach major light-harvesting complex at 2.72 Å resolution, Nature 428 (2004) 287–292.
[11] K.N. Ferreira, T.M. Iverson, K. Maghlaoui, J. Barber, S. Iwata, Architecture of the photosynthetic oxygen-evolving center, Science 303 (2004) 1831–1838.
[12] J. Biesiadka, B. Loll, J. Kern, K.D. Irrgang, A. Zouni, Crystal structure of cyanobacterial photosystem II at 3.2 Å resolution: a closer look at the Mn-cluster, Phys. Chem., Chem. Phys. 6 (2004) 4733–4736.
[13] J. Kern, A. Zouni, P. Franke, W. Schr—der, K.D. Irrgang, Photosystem II subunit composition of cyanobacteria and higher plants, Biochim. Biophys. Acta (submitted for publication).
[14] J. Kern, B. Loll, C. Lüneberg, D. DiFiore, J. Biesiadka, K.D. Irrgang, A. Zouni, Purification, characterisation and crystallisation of photosystem II from *Thermosynechococcus elongatus* cultivated in a new type of photobioreactor, Biochim. Biophys. Acta 1706 (2005) 147–157.
[15] A. Zouni, J. Kern, J. Frank, T. Hellweg, J. Behlke, W. Saenger, K.D. Irrgang, Size determination of cyanobacterial and higher plant Photosystem II by Gel Permeation Chromatography, Light Scattering and Ultracentrifugation, Biochemistry 44 (2005) 4572–4581.
[16] S.C. Straley, W.W. Parson, D.C. Mauzerall, R.K. Clayton, Pigment content and molar extinction coefficients of photochemical reaction centers from *Rhodospeudomonas sphaeroides*, Biochim. Biophys. Acta 305 (1973) 597–609.
[17] R.K. Clayton, B.J. Clayton, Molar extinction coefficients and other properties of an improved reaction center preparation from *Rhodopseudomonas viridis*, Biochim. Biophys. Acta 501 (1978) 478–487.
[18] T. Hiyama, B. Ke, Difference spectra and extinction coefficients of P700, Biochim. Biophys. Acta 267 (1972) 160–171.
[19] H.J. van Gorkom, J.J. Tamminga, J. Haveman, Primary reactions, plastoquinone and fluorescence yield in subchloroplast fragments prepared with deoxycholate, Biochim. Biophys. Acta 347 (1974) 417–438.
[20] P. Gast, P. Hemelrijk, A.J. Hoff, Determination of the number of detergent molecules associated with the reaction center protein isolated from the photosynthetic bacterium *Rhodopseudomonas viridis*. Effects of the amphiphilic molecule 1,2,3-heptanetriol, FEBS Lett. 337 (1994) 39–42.
[21] P. Gast, P.W. Hemelrijk, H.J. Van Gorkom, A.J. Hoff, The association of different detergents with the photosynthetic reaction center protein of *Rhodobacter sphaeroides* R26 and the effects on its photochemistry, Eur. J. Biochem. 239 (1996) 805–809.
[22] F. Müh, J. Rautter, W. Lubitz, Effects of zwitterionic detergents on the primary donor of bacterial reaction centers, Ber. Bunsenges. Phys. Chem. 100 (1996) 1974–1977.
[23] P. Jekow, P. Fromme, H.T. Witt, W. Saenger, Photosystem I from *Synechococcus elongatus*: preparation and crystallization of monomers with varying subunit composition, Biochim. Biophys. Acta 1229 (1995) 115–120.

[24] R.J. Porra, W.A. Thompson, P.E. Kriedemann, Determination of accurate extinction coefficients and simultaneous equations for assaying chlorophyll *a* and *b* extracted with four different solvents: verification of the concentration of chlorophyll standards by atomic absorption spectroscopy, Biochim. Biophys. Acta 975 (1989) 384–394.
[25] P. Hemelrijk, PhD thesis, University of Leiden 1995.
[26] L.K. Hanson, Molecular orbital theory of monomer pigments, in: H. Scheer (Ed.), Chlorophylls, CRC Press, Boca Raton, 1991, pp. 993–1013.
[27] M. Fragata, B. Nordén, T. Kurucsev, Linear dichroism (250–700 nm) of chlorophyll a and pheophytin a oriented in a lamellar phase of glycerylmonooctanoate/H20. Characterization of electronic transitions, Photochem. Photobiol. 47 (1988) 133–143.
[28] D. Sundholm, Comparison of the electronic excitation spectra of chlorophyll a and pheophytin a calculated at density functional theory level, Chem. Phys. Lett. 317 (2000) 545–552.
[29] C. Eijckelhoff, J.P. Dekker, A routine method to determine the chlorophyll a, pheophytin a and β-carotene contents of isolated Photosystem II reaction center complexes, Photosynth. Res. 52 (1997) 69–73.
[30] C. Flemming. diploma thesis, Technical University Berlin 1996.
[31] L.N. Duysens, The flattening of the absorption spectrum of suspensions, as compared to that of solutions, Biochim. Biophys. Acta 19 (1956) 1–12.
[32] P. Rosevear, T. VanAken, J. Baxter, S. Ferguson-Miller, Alkyl glycoside detergents: a simpler synthesis and their effects on kinetic and physical properties of cytochrome *c* oxidase, Biochemistry 19 (1980) 4108–4115.
[33] K. Kalyanasundaram, J.K. Thomas, Environmental effects on vibronic band intensities in pyrene monomer fluorescence and their application in studies of micellar systems, J. Am. Chem. Soc. 99 (1977) 2039–2044.